

# HEAVY IONS INTERPRETATION OF HIGHEST ENERGY COSMIC RAYS

STEVE REUCROFT

*Department of Physics, Northeastern University,  
Boston, MA 02115, USA*

A brief review of the energy spectrum of primary cosmic rays above  $10^{10}$  eV and the measurement techniques used to investigate the ultra high energy ones is given. This is followed by a discussion of the atmospheric shower profile of the highest energy event observed using the Fly's Eye detector. Finally, cosmic ray simulation tools are discussed and used to investigate the heavy ion interpretation of the highest energy primary. The best way to contribute further to the understanding of this issue is by the collection of new and better data.

## 1 Cosmic Ray Energy Spectrum

The cosmic ray (CR) spectrum above  $10^{10}$  eV (where the Sun's magnetic field is no longer a concern) can be described by a series of power laws with the flux falling about 3 orders of magnitude for each decade increase in energy,<sup>1</sup> see Fig. 1. Above  $10^{14}$  eV, the flux becomes so low that direct measurements using sophisticated equipment on satellites or high altitude balloons are limited in detector area and in exposure time. Ground-based experiments with large apertures make such a low flux observable after a magnification effect in the upper atmosphere: the incident cosmic radiation interacts with atomic nuclei of the air molecules and produces extensive air showers which spread out over large areas. Continuously running using ingenious installations has raised the maximum observed primary particle energy to higher than  $10^{20}$  eV.<sup>2</sup>

While theoretical subtleties surrounding CR acceleration provide ample material for discussion, the debate about the origin of CRs up to the knee ( $\sim 10^{15.5}$  eV) has reached a consensus that they are produced in supernova explosions.<sup>3</sup> The change of the spectral index (from  $-2.7$  to  $-3.0$ ) near the knee, presumably reflects a change in origin and the takeover of another, yet unclear type of source. The spectrum steepens further to  $-3.3$  above  $\sim 10^{17.7}$  eV (the dip) and then flattens to an index of  $-2.7$  at  $\sim 10^{18.5}$  eV (the ankle). A very widely held interpretation of the modulation features is that above the ankle a new population of CRs with extragalactic origin begins to dominate the more steeply falling Galactic population.<sup>a</sup> The origin of the extragalactic channel is somewhat mysterious.

CRs do not travel unhindered through intergalactic space, as there are several processes that can degrade the particles' energy. In particular, the thermal photon background becomes highly blue shifted for ultrarelativistic protons. The reaction sequence  $p\gamma \rightarrow \Delta^+ \rightarrow \pi^0 p$  effectively degrades the primary proton energy providing a strong constraint on the proximity of CR-sources, a phenomenon known as the Greisen-Zatsepin-Kuz'min (GZK) cutoff.<sup>5</sup> The energy attenuation length of protons<sup>6</sup> is shown in Fig. 2. A heavy nucleus undergoes photodisintegration in the microwave and infra-red backgrounds; as a result, iron nuclei do not survive fragmentation over

---

<sup>a</sup>This hypothesis is supported by AGASA data.<sup>4</sup>

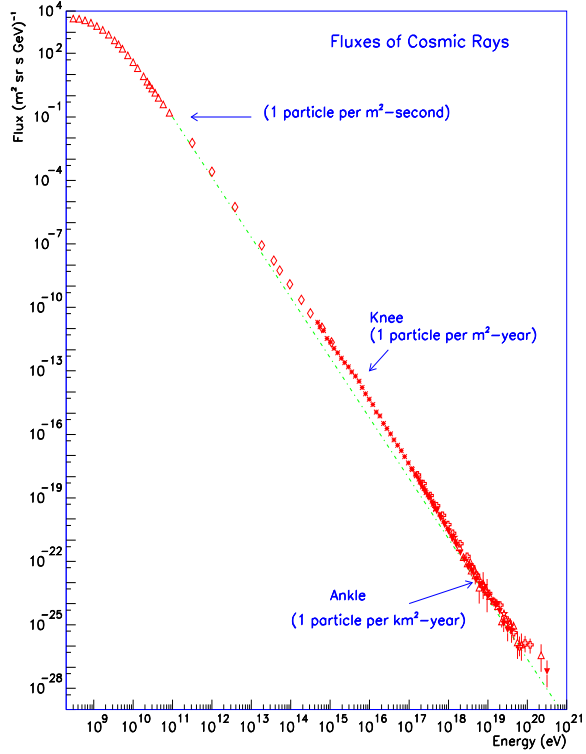


Figure 1: Cosmic ray energy spectrum.

comparable distances.<sup>7</sup> Ultra high energy gamma rays would travel even shorter paths due to pair production on radio photons.<sup>8</sup> Therefore, if the CR sources are all at cosmological distances, the observed spectrum must virtually end with the GZK cutoff at  $E \approx 8 \times 10^{19}$  eV. The spectral cutoff is less sharp for nearby sources (within 50 Mpc or so).<sup>9</sup> The arrival directions of the trans-GZK events are distributed widely over the sky, with no plausible optical counterparts (such as sources in the Galactic Plane or in the Local Supercluster). Furthermore, the data are consistent with an isotropic distribution of sources in sharp contrast to the anisotropic distribution of light within 50 Mpc.<sup>10</sup>

The difficulties encountered by conventional acceleration mechanisms in accelerating particles to the highest observed energies have motivated suggestions that the underlying production mechanism could be of non-acceleration nature. Namely, charged and neutral primaries, mainly light mesons (pions) together with a small fraction (3%) of nucleons, might be produced at extremely high energy by decay of supermassive elementary  $X$  particles ( $m_X \sim 10^{22} - 10^{28}$  eV).<sup>11</sup> However, if this were the case, the observed spectrum should be dominated by gamma rays and neutrinos, in contrast to current observation!<sup>12</sup> Alternative explanations involve undiscovered neutral hadrons with masses above a few GeV,<sup>13</sup> neutrinos producing nucleons and photons via resonant  $Z$ -production with the relic neutrino background,<sup>14</sup> or else neutrinos attaining cross sections in the millibarn range above the electroweak scale.<sup>15</sup> If neutrinos/neutral-hadrons are primaries, they should point back to their sources, thereby enabling point source astronomy for the most energetic sources of flux at and above the GZK energy. However, the current CR-sample does not show significant angular correlation with powerful high-redshift sources.<sup>16</sup>

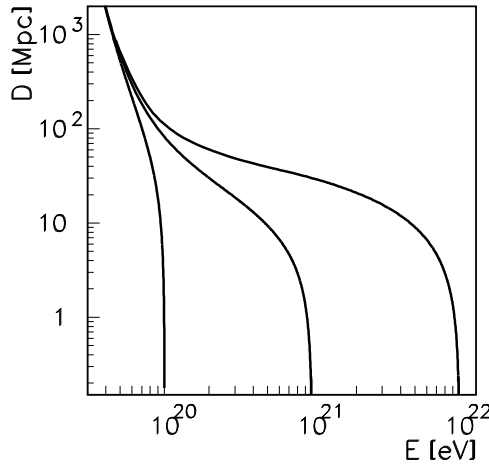


Figure 2: Energy attenuation length of nucleons in the intergalactic medium. Notice that independently of the initial energy of the nucleon, the mean energy values approach to 100 EeV after a distance of approx 100 Mpc.

## 2 Measurement Techniques

There are two major techniques used in the detection of ultra high energy CRs. The first one is to build an array of sensors (scintillators, water Cerenkov tanks, muon detectors) spread over a large area. The detectors count the particle densities at any given moment, thus sampling the shower particles hitting the ground. By means of the ground lateral distributions of the shower one can deduce the direction, the energy and possibly the identity of the primary CR. The Akeno Giant Air Shower Array (AGASA) is the largest array so far constructed to measure extensive air showers. This array comprise 111 scintillation detectors each of  $2.2 \text{ m}^2$  spread over a grid of  $100 \text{ km}^2$  with 1 km spacing.<sup>17</sup> The array detectors are connected and controlled through a sophisticated optical fibre network. The array also contains a number of shielded scintillation detectors which provide information of the muon content of the showers. The second technique, pioneered by the University of Utah's Fly's Eye detector,<sup>18</sup> consists in studying the longitudinal development of extensive air showers by detecting the fluorescence light produced by the interactions of the charged secondaries. Measurement of atmospheric fluorescence is possible only on clear, dark nights. Since mid-1998 a successor to the Fly's Eye instrument, called Hi-Res, has started taken data at the Dugway site.<sup>19</sup> In its final form it is expected to have a time-average aperture of  $340 \text{ km}^2 \text{ sr}$  at  $10^{19} \text{ eV}$  and  $1000 \text{ km}^2$  at  $10^{20} \text{ eV}$ .

The Auger experiment has been conceived to measure the properties of cosmic rays above  $10^{19} \text{ eV}$  with unprecedented statistical precision.<sup>20</sup> The Observatory will consist of two sites (in the Northern and Southern hemispheres) designed to work in a hybrid detection mode, each covering an area of  $3000 \text{ km}^2$  with 1600 particle detectors overviewed by 4 fluorescence detectors. Surface array stations are water Cerenkov detectors (a cylindrical tank of  $10 \text{ m}^2$  top surface and 1.2 m height, filled with filtered water and lined with a highly reflective material, the Cerenkov radiation is detected by 3 photomultiplier-tubes installed at the top) spaced 1.5 km from each other in an hexagonal grid. These stations will operate on battery-backed solar power and will communicate with a central station by using wireless local area network radio links. Event timing will be provided through global positioning system (GPS) receivers. Of course, the hybrid reconstruction (see Fig. 3) will be extremely valuable for energy calibration, but such "golden" events are expected to be less than 10% of the total event rate.

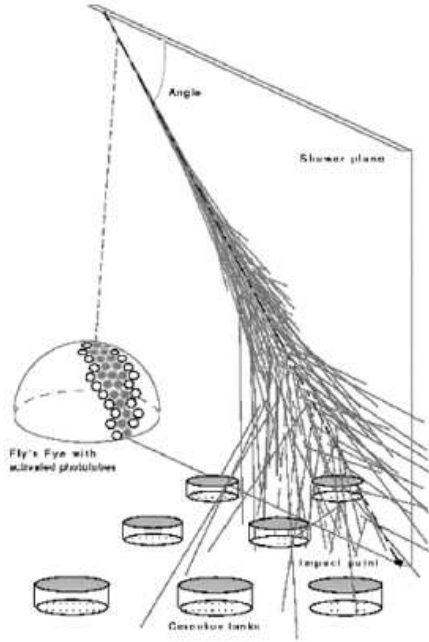


Figure 3: Schematic representation of the operation of a hybrid air shower detector.

It is worth mentioning that an array of ground-based detectors is ideally suited for involving school students and their teachers in cosmic ray research. This has been proposed several times (for example, SCROD<sup>21,22</sup>).

### 3 Shower Profile of Highest Energy Fly's Eye Event

The Fly's Eye observes an air shower as a nitrogen fluorescence light source which moves at the speed of light along the path of a high energy particle traversing the atmosphere.<sup>18</sup> In other words, it directly detects the longitudinal development of the air cascade. The simulation of the shower evolution depends sensitively on the first few interactions, necessarily related to the quality of our “understanding” of hadronic collisions. The well known codes QGSJET<sup>23</sup> and SIBYLL<sup>24</sup> represent two of the best simulation tools to model hadronic interactions at the highest energies. The underlying idea behind SIBYLL is that the increase in the cross section is driven by the production of minijets.<sup>24</sup> The probability distribution for obtaining  $N$  jet pairs (with  $p_T^{\text{jet}} > p_T^{\text{min}}$ , where  $p_T^{\text{min}}$  is a sharp threshold on the transverse momentum below which hard interactions are neglected) in a collision at energy  $\sqrt{s}$  is computed regarding elastic  $pp$  or  $p\bar{p}$  scattering as a diffractive shadow scattering associated with inelastic processes. The algorithms are tuned to reproduce the central and fragmentation regions data up to  $p\bar{p}$  collider energies, and with no further adjustments they are extrapolated several orders of magnitude. On the other hand, in QGSJET the theory is formulated entirely in terms of Pomeron exchanges. The basic idea is to replace the soft Pomeron by a so-called “semihard Pomeron”, which is defined to be an ordinary soft Pomeron with the middle piece replaced by a QCD parton ladder. Thus, minijets will emerge as a part of the “semihard Pomeron”, which is itself the controlling mechanism for the whole interaction.<sup>23</sup> The different approaches used in both codes to model the underlying physics show clear differences in cross sections (see Fig. 4) and multiplicity predictions which increase with rising energy.<sup>25</sup> As can be seen in Fig. 5, for proton-induced showers, the differences become washed out as the shower front gets closer to the ground.

Nevertheless, the footprints of the first hadronic collisions are still present in the longitudinal

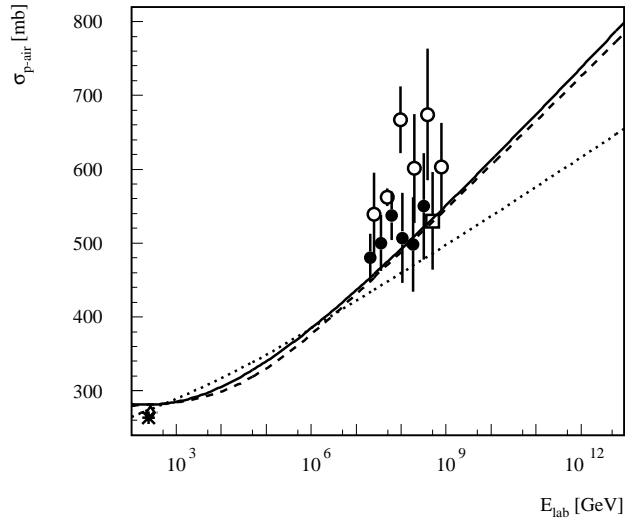


Figure 4:  $p$ -air cross sections of SIBYLL (dashed line), QGSJET (dots), and AIRES (solid line) superimposed on data obtained from collider experiments and cosmic ray experiments.<sup>25</sup>

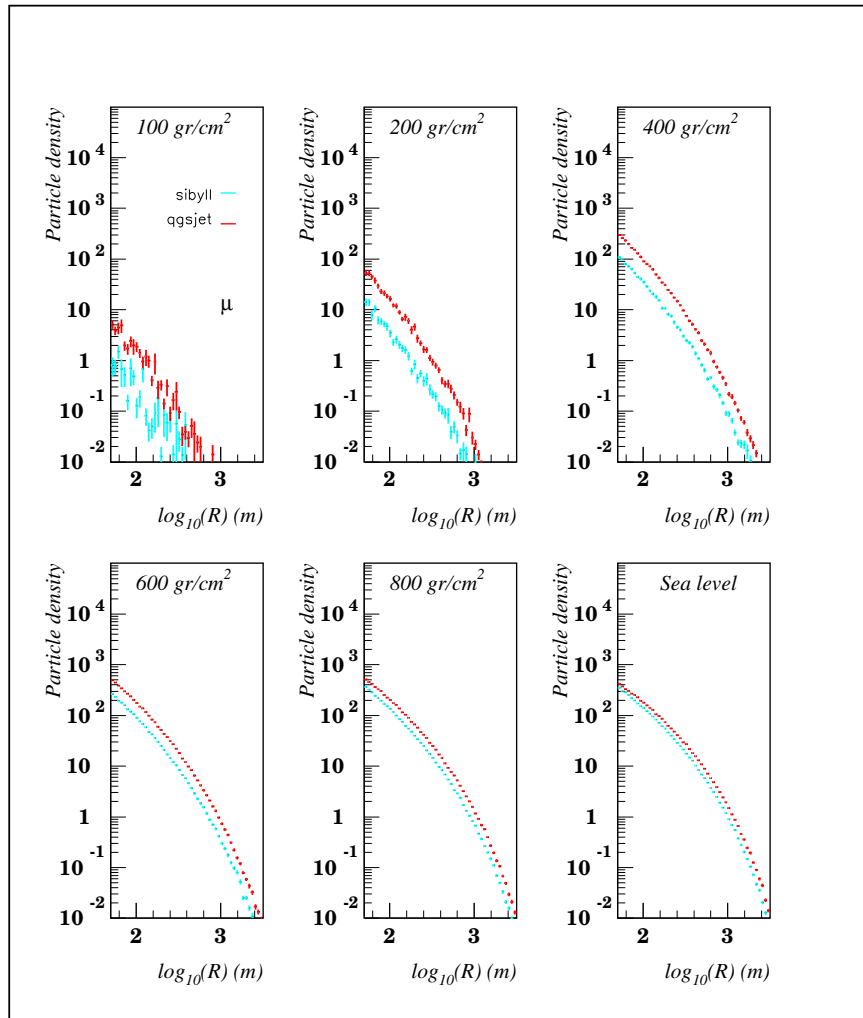


Figure 5: Comparison of muon lateral distributions at different atmospheric depths.  $E_p = 10$  EeV.<sup>26</sup>

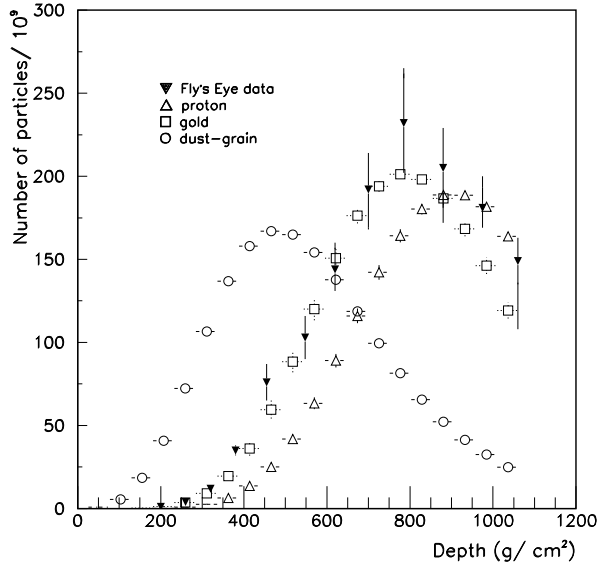


Figure 6: Longitudinal development of 300 EeV showers from different primary species together with the data of the highest energy event recorded by Fly's Eye.<sup>29</sup>

development. In Fig. 6 we show the atmospheric shower profile of 300 EeV showers induced by a proton, a gold-nucleus and a dust grain<sup>b</sup> obtained after Monte Carlo simulation with the program AIRES (version 2.2.1).<sup>28</sup> SIBYLL was used to generate hadronic interactions above 200 GeV. The simulated results are superimposed over the experimental data of the highest energy Fly's Eye event.<sup>30</sup> It is clearly seen that the gold-nucleus longitudinal development better reproduces the data than a proton or a dust grain. However, this is not the case when the hadronic collisions are modelled with QGSJET. As can be seen in Fig. 7, in this case a medium mass nucleus likely fits the Fly's Eye data.

All in all, the primary chemical composition remains hidden by the hadronic interaction model. In light of this, in the next section we examine in more detail the speculative case of superheavy nuclei.

#### 4 Superheavy Nuclei

It has been generally thought that  $^{56}\text{Fe}$  is a significant end product of stellar evolution and higher mass nuclei are rare in the cosmic radiation. Strictly speaking, the atomic abundances of middle-weight ( $60 \leq A < 100$ ) and heavy-weight ( $A > 100$ ) elements are approximately 3 and 5 orders of magnitude lower, respectively, than that of the iron group.<sup>32</sup> The synthesis of the stable super-heavy nuclides is classically ascribed to three different stellar mechanisms referred to as the s-, r-, and p-processes. The s-process results from the production of neutrons and their capture by pre-existing seed nuclei on time scales longer than most  $\beta$ -decay lifetimes. There is observational evidence that such a kind of process is presently at work in a variety of chemically peculiar Red Giants<sup>33</sup> and in special objects like FG Sagittae<sup>34</sup> or SN1987A.<sup>35</sup> The abundance of well developed nuclides peaks at mass numbers  $A = 138$  and  $A = 208$ . The neutron-rich (or r-nuclides) are synthesized when seed nuclei are subjected to a very intense neutron flux so that  $\beta$ -decays near the line of stability are far too slow to compete with the neutron capture. It has long been thought that appropriate r-process conditions could be found in the hot ( $T \geq 10^{10} \text{ K}$ ) and dense ( $\rho \sim 10^{10} - 10^{11} \text{ g/cm}^3$ ) neutron-rich (neutronized) material located behind the

<sup>b</sup>A very massive particle containing  $10^7$  nucleons.<sup>27</sup>

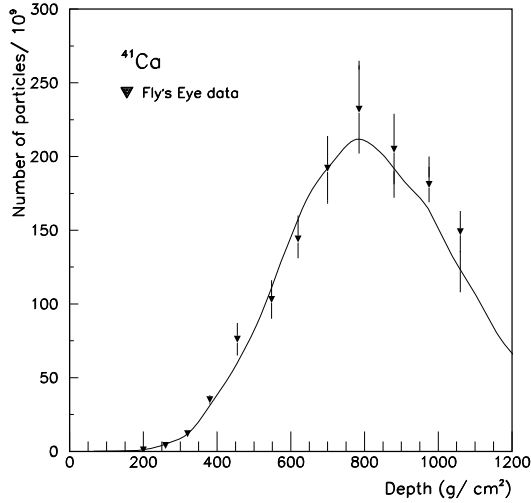


Figure 7: Atmospheric cascade development of 300 EeV calcium-nucleus together with Fly's Eye data.<sup>31</sup>

outgoing shock in a type II supernova event.<sup>36</sup> Its abundance distribution peaks at  $A = 130$  and  $A = 195$ . The neutron-deficient (or p-nuclides) are 100-1000 times less abundant than the corresponding more neutron rich isobars, while their distribution roughly parallels the s- and r-nuclides abundance curve. It is quite clear that these nuclides cannot be made by neutron capture processes. It is generally believed that they are produced from existing seed nuclei of the s- or r-type by addition of protons (radiative proton captures), or by removal of neutrons (neutron photodisintegration). The explosion of the H-rich envelopes of type II supernovae has long been held responsible for the synthesis of these nuclides.<sup>32</sup>

Putting all this together, starbursts appear as the natural sources able to produce relativistic super-heavy nuclei. These astrophysical environments are supposed to comprise a considerable population of O and Red Giant stars,<sup>37</sup> and we believe the supernovae rate<sup>38</sup> is as high as 0.2-0.3 yr<sup>-1</sup>. It was recently put forward that within this type of galaxies, iron nuclei can be accelerated to extremely high energies if a two step process is invoked.<sup>39</sup> In a first stage, ions are diffusively accelerated up to a few PeV at single supernova shock waves in the nuclear region of the galaxy.<sup>3</sup> Since the cosmic ray outflow is convection dominated, the typical residence time of the nuclei in the starburst results in  $t \sim 1 \times 10^{11}$  s. Thus, the total path traveled is substantially shorter than the mean free path (which scales as  $A^{-2/3}$ ) of a super-heavy nucleus. Those which are able to escape from the central region without suffering catastrophic interactions could be eventually re-accelerated to superhigh energies at the terminal shocks of galactic superwinds generated by the starburst. The mechanism efficiently improves as the charge number  $Z$  of the particle is increased. For this second step in the acceleration process, the photon field energy density drops to values of the order of the cosmic background radiation (we are now far from the starburst region).

The dominant mechanism for energy losses in the bath of the universal cosmic radiation is the photodisintegration process. The disintegration rate  $R$  (in the system of reference where the microwave background radiation is at 2.73K) of an extremely high energy nucleus with Lorentz factor  $\Gamma$ , propagating through an isotropic soft photon background  $n(\epsilon)$  reads<sup>40</sup>

$$R = \frac{1}{2\Gamma^2} \int_0^\infty d\epsilon \frac{n(\epsilon)}{\epsilon^2} \int_0^{2\Gamma\epsilon} d\epsilon' \epsilon' \sigma(\epsilon'), \quad (1)$$

where  $\sigma$  stands for the total photon absorption cross section. Primed quantities refer to the

Table 1: Giant dipole resonance parameters

$\epsilon_0$ [MeV]	$\sigma_0$ [mb]	$\Gamma_0$ [MeV]
13.15	255	2.9
13.90	365	4.0

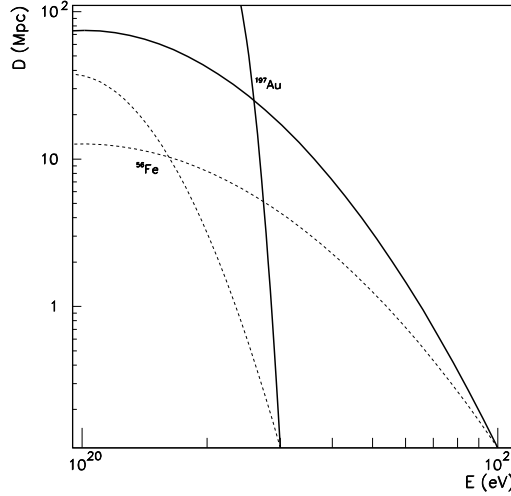


Figure 8: Energy attenuation length of gold (solid) and iron (dashed) nuclei in the intergalactic medium.

rest frame of the nucleus. The total photon absorption cross section is characterized by a broad maximum, designated as the giant resonance, located at an energy of 12-20 MeV depending on the nucleus under consideration. For the medium and heavy nuclei,  $A \geq 50$ , the cross section can be well represented by a single, or in the case of the deformed nuclei, by the superposition of two Lorentzian curves of the form

$$\sigma(\epsilon') = \sigma_0 \frac{\epsilon'^2 \Gamma_0^2}{(\epsilon_0^2 - \epsilon'^2)^2 + \epsilon'^2 \Gamma_0^2}. \quad (2)$$

In order to make some estimates, hereafter we refer our calculations to a gold nucleus (the resonance parameters are listed in table I).<sup>41</sup> Figure 8 shows the energy attenuation length of a gold nucleus due to interactions with the infrared and microwave backgrounds.<sup>42</sup> For comparison, we also show the energy attenuation length of an iron nucleus. We can conclude that despite the fact the abundances of superheavy nuclei are around 4 orders of magnitude lower respective to the iron group, the volume for the potential sources of extremely high energy superheavy nuclei ( $E \approx 300$  EeV) increases substantially.

## 5 Conclusions

The energy spectrum of primary cosmic rays above  $10^{10}$  eV has several compelling features. Perhaps the most impressive is the apparent occurrence of events above the GZK cutoff. This issue has been studied using simulation techniques and leads to a plausible interpretation of the highest energy cosmic ray event as due to the atmospheric interaction of an energetic heavy ion. The only reliable way to contribute further to the understanding of this issue is by the collection of new and better data in future experiments.

## Acknowledgments

I acknowledge crucial help from my friend and colleague Luis Anchordoqui; he provided me with all the figures and most of the text! I thank Bill Marciano and Sebastian White for organizing such an interesting and eclectic workshop and I am in awe of Antonino Zichichi for providing Science with such an amazing resource as the one at Erice. Finally, I am grateful to the US National Science Foundation for financial support.

## References

1. For comprehensive reviews the reader is referred to, J. Cronin, T. K. Gaisser and S. P. Swordy, *Sci. Amer.* **276** 44 (1997); S. Yoshida, and H. Dai, *J. Phys. G* **24**, 905 (1998); M. Nagano and A. A. Watson, *Rev. Mod. Phys.* **72**, 689 (2000).
2. J. Linsley, *Phys. Rev. Lett.* **10**, 146 (1963); M. A. Lawrence, R. J. O. Reid and A. A. Watson, *J. Phys. G* **17**, 773 (1991); M. Takeda *et al.*, *Phys. Rev. Lett.* **81**, 1163 (1998); D. J. Bird *et al.*, *Phys. Rev. Lett.* **71**, 3491 (1993); E. Antonov *et al.*, *JETP Lett.* **69**, 650 (1999).
3. P. O. Lagage and C. J. Cesarsky, *Astron. Astrophys.* **118**, 223 (1983); P. L. Biermann, *Astron. Astrophys.* **271**, 649 (1993).
4. N. Hayashida *et al.*, *Astropart. Phys.* **10**, 303 (1999).
5. K. Greisen, *Phys Rev. Lett.* **16**, 748 (1966); G.T. Zatsepin and V.A. Kuz'min, *Pis'ma Zh. Eksp. Teor. Fiz.* **4**, 114 (1966) [*JETP Lett.* **4**, 78 (1966)].
6. L.A. Anchordoqui, M.T. Dova, L.N. Epele, and J.D. Swain *Phys. Rev. D* **55**, 7356 (1997).
7. J. L. Puget, F. W. Stecker and J. H. Bredekamp, *Astrophys. J.* **205**, 638 (1976). Updated in, L. A. Anchordoqui, M. T. Dova, L. N. Epele, and J. D. Swain, *Phys. Rev. D* **57**, 7103 (1998); L. N. Epele and E. Roulet, *JHEP* **10**, 009 (1998); F. W. Stecker and M. H. Salamon, *Astrophys. J.* **512**, 521 (1999).
8. R. J. Protheroe and P. Johnson, *Astropart. Phys.* **4**, 253 (1996).
9. G. R. Farrar, T. Piran, *Phys. Rev. Lett.* **84**, 3527 (2000); P.L. Biermann, E.J. Ahn, G. Medina Tanco, T. Stanev *Nucl. Phys. B (Proc.Suppl.)* **87**, 417 (2000); L. A. Anchordoqui, H. Goldberg, T. J. Weiler, *Phys. Rev. Lett.* **87**, 081101 (2001); L. Anchordoqui, H. Goldberg, S. Reucroft, and J. Swain, *Phys. Rev. D* **64**, 123004 (2001).
10. E. Waxman, K. B. Fisher and T. Piran, *Astrophys. J.* **483**, 1 (1997); M. Hillas, *Nature* **395**, 15 (1998).
11. P. Bhattacharjee and G. Sigl, *Phys. Rep.* **327** 109 (2000).
12. M. Ave, J. A. Hinton, R. A. Vazquez and A. A. Watson, *Phys. Rev. Lett.* **85**, 2244 (2000).
13. G. R. Farrar, *Phys. Rev. Lett.* **76**, 4111 (1996); D. J. H. Chung, G. R. Farrar and E. W. Kolb, *Phys. Rev. D* **57**, 4696 (1998).
14. T. J. Weiler, *Phys. Rev. Lett.* **49**, 234 (1982); *Astrophys. J.* **285**, 495 (1984); *Astropart. Phys.* **11**, 303 (1999); D. Fargion, B. Mele and A. Salis, *Astrophys. J.* **517**, 725 (1999).
15. S. Nussinov and R. Shrock, *Phys. Rev. D* **59**, 105002 (1999); G. Domokos and S. Kovács-Domokos, *Phys. Rev. Lett.* **82**, 1366 (1999); P. Jain, D. W. McKay, S. Panda, and J. P. Ralston, *Phys. Lett. B* **484**, 267 (2000); C. Tyler, A. Olinto and G. Sigl, *Phys. Rev. D* **63**, 055001 (2001); L. Anchordoqui, H. Goldberg, T. McCauley, T. Paul, S. Reucroft and J. Swain [hep-ph/0011097]; A. Jain, P. Jain, D. W. McKay and J. P. Ralston [hep-ph/0011310].
16. G. R. Farrar, P. L. Biermann, *Phys. Rev. Lett.* **81**, 3579 (1998); G. Sigl *et al.*, *Phys. Rev. D* **63**, 081302 (2001); A. Virmani, S. Bhattacharya, P. Jain, S. Razzaque, J. P. Ralston, and D. W. McKay, [astro-ph/0010235].

17. N. Chiba *et al.*, Nucl. Instrum. Meth. A **311**, 338 (1992); H. Ohoka, S. Yoshida and M. Takeda [AGASA Collaboration], Nucl. Instrum. Meth. A **385**, 268 (1997).
18. R. M. Baltrusaitis *et al.*, Nucl. Inst. Methods Phys. Res., Sect. A **240**, 410 (1985).
19. P. Sokolsky, AIP Conference Proceedings **433**, 65 (1998).
20. <http://www.auger.org/admin/>
21. <http://hepnt.physics.neu.edu/scrod/index.html>
22. L. A. Anchordoqui, J. Cook, M. Gabour, N. Kirsch, J. MacLeod, T. P. McCauley, Y. Musienko, T. C. Paul, S. Reucroft, J. D. Swain, R. Terry, [hep-ex/0106002].
23. N. N. Kalmykov, S. S. Ostapchenko, A. I. Pavlov, Nucl. Phys. B (Proc. Supp.) **B52**, 17 (1997).
24. R. S. Fletcher, T. K. Gaisser, P. Lipari and T. Stanev, Phys. Rev. D **50**, 5710 (1994).
25. L. A. Anchordoqui, M. T. Dova, L. N. Epele and S. J. Sciutto, Phys. Rev. D **59**, 094003 (1999).
26. L. A. Anchordoqui, [astro-ph/9812445].
27. L. A. Anchordoqui, Phys. Rev. D **61**, 087302 (2000).
28. S. J. Sciutto, in *Proc. XXVI International Cosmic Ray Conference*, (Edts. D. Kieda, M. Salamon, and B. Dingus, Salt Lake City, Utah, 1999) vol.1, p.411.
29. L. A. Anchordoqui, M. T. Dova, T. P. McCauley, T. Paul, S. Reucroft, and J. D. Swain, Nucl. Phys. B (Proc. Suppl.) **97**, 203 (2001).
30. D. J. Bird *et al.*, Astrophys. J. **441**, 144 (1995).
31. L. A. Anchordoqui, M. Kirasirova, T. P. McCauley, S. Reucroft, J. D. Swain, Phys. Lett. B **492**, 237 (2000).
32. E. M. Burbidge, G. R. Burbidge, W. A. Fowler, and F. Hoyle, Rev. Mod. Phys. **29**, 547 (1957).
33. V. V. Smith, AIP Conference Proceedings **183**, 200 (1989).
34. G. E. Langer, R. P. Kraft, K. S. Anderson, Astrophys. J. **189**, 509 (1974).
35. P. A. Mazzali, L. B. Lucy, K. Butler, Astron. Astrophys. **258**, 399 (1992).
36. M. D. Delano and A. G. W. Cameron, Astrophys. Space. Sci. **10**, 203 (1971); W. Hillebrandt, K. Takahashi and T. Kodama, Astron. Astrophys. **52**, 63 (1976).
37. S. Sakai and B. Madore, [astro-ph/9906484].
38. See for instance, T. W. B. Muxlow *et al.*, Mont. Not. Roc. Astron. Soc. **266**, 455 (1994); J. S. Ulvestad and R. J. Antonucci, Astrophys. J. **448**, 621 (1997); D. A. Forbes *et al.*, Astrophys. J. **406**, L11 (1993); R. de Grijs *et al.*, [astro-ph/9909044].
39. L. A. Anchordoqui, G. E. Romero, and J. A. Combi, Phys. Rev. D **60**, 10300 (1999).
40. F. W. Stecker, Phys. Rev. D **180**, 1264 (1969).
41. E. G. Fuller and M. S. Weiss, Phys. Rev. **112**, 560 (1958).
42. L. A. Anchordoqui, M. T. Dova, T. P. McCauley, S. Reucroft, and J. D. Swain, Phys. Lett. B **482**, 343 (2000).